Mon. Not. R. Astron. Soc. **000**, 000–000 (0000) Printed 27 June 2008 (MN LATEX style file v2.2)

Two New Large Separation Gravitational Lenses from SDSS

V. Belokurov [1], N.W. Evans [1], P.C. Hewett [1], A. Moiseev[2], R.G. McMahon[1], S.F. Sanchez[3] and L.J. King[1]

[1] *Institute of Astronomy, University of Cambridge*
[2] *Special Astrophysical Observatory, Nizhniy Arkhyz, Karachaevo-Cherkessiya, Russia*
[3] *Centro Astronomico Hispano Aleman de Calar Alto (CSIC-MPIA), E4004 Almera, Spain*

27 June 2008

ABSTRACT

We present discovery images, together with follow-up imaging and spectroscopy, of two large separation gravitational lenses found by our survey for wide arcs (the CASSOWARY). The survey exploits the multicolour photometry of the Sloan Digital Sky Survey to find multiple blue components around red galaxies. CASSOWARY 2 (or "the Cheshire Cat") is composed of two massive early-type galaxies at $z = 0.426$ and 0.432 respectively lensing two background sources, the first a star-forming galaxy at $z = 0.97$ and the second a high redshift galaxy ($z > 1.4$). There are at least 3 images of the former source and probably 4 or more of the latter, arranged in two giant arcs. The mass enclosed within the larger arc of radius $\sim 11''$ is $\sim 33 \times 10^{12}$ M$_\odot$. CASSOWARY 3 comprises an arc of three bright images of a $z = 0.725$ source, lensed by a foreground elliptical at $z = 0.274$. The radius of the arc is $\sim 4''$ and the enclosed mass is $\sim 2.4 \times 10^{12}$ M$_\odot$. Together with earlier discoveries like the Cosmic Horseshoe and the 8 O'Clock Arc, these new lenses help probe the very high end of the galaxy mass function – the regime intermediate between the arcsecond separation lenses of typical strong lensing and cluster lensing.

Key words: Gravitational lensing – galaxies: structure – galaxies:evolution

1 INTRODUCTION

Very recently, a number of large separation gravitational lenses have been found in data from the Sloan Digital Sky Survey (SDSS). This includes: the 8 O'clock Arc, which is a Lyman Break galaxy lensed into three images merging into an extended arc (Allam et al. 2006), the Cosmic Horseshoe, which is a star-forming galaxy lensed into an almost complete Einstein ring of diameter $10''$ (Belokurov et al. 2007), and the strongly lensed post-starburst galaxy of Shin et al. (2008).

These discoveries prompted us to set up the *The CAmbridge Sloan Survey Of Wide ARcs in the skY* (CASSOWARY [1]). The aim is to carry out systematic searches for wide separation gravitational lens systems, looking for multiple, blue companions around massive ellipticals in the SDSS object catalogue. Typically, the target systems correspond to lensing of $z \gtrsim 0.5$ star-forming galaxies by luminous red galaxies and brightest cluster galaxies. Here, we present details of two new gravitational lens systems, for which we have obtained follow-up on a number of telescopes, including the 6 m at the *Special Astrophysical Observatory* (SAO), the 3.5 m at *Calar Alto*, and the 2.5 m *Isaac Newton* (INT) and the 4.2 m *William Herschel Telescopes* (WHT) at La Palma.

Previous search strategies typically target smaller separation lenses, in which the images are unresolved by SDSS. For example, Inada et al. (2003b) and Johnston et al. (2003) searched through spectroscopically identified quasars, looking for evidence for extended sources corresponding to unresolved, multiple images, whilst Johnston et al. (2003) and Willis et al. (2005) used the spectroscopic database to look for emission lines of high redshift objects within the spectrum of lower redshift early-type galaxies.

Although wide separation lenses ($\gtrsim 3''$) are comparatively unexplored, they are interesting for a number of reasons. First, wide separation lenses are a probe of the high mass end of the galaxy mass function. The Einstein radius is typically a few effective radii where the matter distribution is dominated by dark matter. Second, the source is often highly magnified and thus provides us with a sample of the brightest galaxies known at high redshifts – for example, the Cosmic Horseshoe or CASSOWARY 1 (Belokurov et al. 2007; Dye et al. 2008). Third, the modelling of such systems is relatively clean. The positioning of the images well outside the effective radius of the lens means that their properties, particularly their brightnesses, can be measured with high accuracy. Fourth, the frequency of large separation lenses provides constraints on models of structure formation. For example, fossil groups, in which bright galaxies have merged via dynamical friction to leave a single very massive object, are amongst the lenses targeted by the CAS-

[1] http://www.ast.cam.ac.uk/research/cassowary/

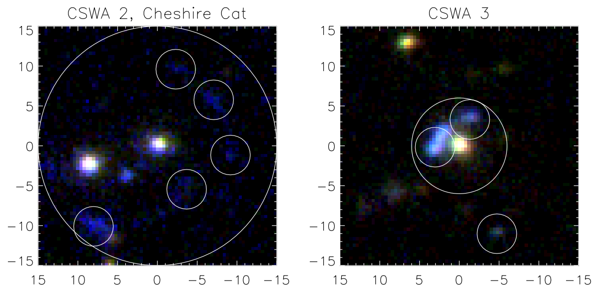

Figure 1. SDSS g, r, i composite images of CSWA 2 and CSWA 3. The large circle marks the search area around the primary, the small circles show locations of blue companions selected by our cuts. The horizontal and vertical scales are relative right ascension and declination in arcseconds.

SOWARY search. Finally, the unusual morphologies of some wide separation lenses are also fascinating from the perspective of the theory of gravitational lensing (Shin & Evans 2008; Werner et al. 2008).

The paper is arranged as follows. §2 presents our general methodology, whilst §3 and §4 presents our two new gravitational lenses in turn – CASSOWARY 2 and CASSOWARY 3 (henceforth CSWA 2 and CSWA 3) – describing our follow-up data, our modelling and predictions. They are the second and third of the CASSOWARY lenses, as the Cosmic Horseshoe is CSWA 1. Finally, §5 summarizes our conclusions and future prospects.

2 METHODOLOGY

2.1 Selection of the Lenses

At its simplest level, our algorithm searches for blue companions to luminous red galaxies. We have already used a precursor of the algorithm to identify the Cosmic Horseshoe (Belokurov et al. 2007), and similar methods have been used recently by Kubik (2007) and Shin et al. (2008). Here, we use a variant of the criteria of Eisenstein et al. (2001) to identify luminous red galaxies (LRGs) in SDSS's `Galaxy` table. Our cuts are slightly changed to include fainter and less red objects than classical LRGs, as we are primarily interested in early-type massive galaxies as opposed to the LRGs themselves. We then use SDSS's `Neighbors` table to select objects with $g - r < 0.6$ and $19 < r < 23.5$ within $30''$ radius. Some standard photometry flags were also used to remove artifacts. For each lens galaxy, we calculate the total number of arc candidates and the mean values of their distance, apparent magnitude, colour and surface brightness. We apply cuts to search for very bright arcs resolved into multiple components at a similar radius from the lensing object. As the lens is assumed to be a single galaxy with modest shear, the images should be all at about the same distance from the primary and so the distance dispersion should be small. The arcs are required to be bright and to have at least two components of comparable magnitude. We also ensure that, for each lens, the arcs are bluer than the typical physical companions that are expected. Finally, we require that the surface brightness of the arc not be too bright or too faint. The brighter objects are typically foreground galaxies and the fainter are typically tidal arms and bridges common in interacting galaxies.

Our experimentation with various combinations of selection cuts will be described in detail elsewhere (Belokurov et al., in preparation). Here, we concentrate on two particularly interesting systems – illustrated in Fig. 1 – for which we have already obtained deeper imaging and spectroscopy, confirming the gravitational lensing hypothesis.

2.2 Structural Parameters and Environment of the Lenses

In Fig. 2, we present RGB composites for CSWA 2 and 3 made from U, g, i in the case of INT imaging and g, r, i in the case of SDSS imaging. A zoom-in of the g (or R) band image for CSWA 2 (or CSWA 3) is shown in the second column. We then mask the arcs in the g band to identify the lens population, which is modelled using `GALFIT` [2] (Peng et al. 2002). We use a field star to define the PSF and fix the sky levels from aperture photometry of stars around each lens. Models of the foreground galaxies (and occasional star) are shown in red in the third column, whilst the residuals – that is, primarily the arcs – are shown in blue. The red dotted lines show the major axes of the lens galaxies. The fourth panel shows the greyscale image with the foreground population subtracted, together with the best-fitting ellipses to the arcs. These are used to extract the approximate Einstein radii. Table 1 gives the basic observational data for CSWA 2 and CSWA 3 lenses. The total magnitudes for the lenses and the arcs are given in the g and i bands on the SDSS AB system. The i band images of the lensing galaxies have the highest signal-to-noise ratio, and so they are used to extract the effective radii using a standard de Vaucouleurs fit. Follow-up spectroscopy is used to determine the lens redshift for CSWA 2 and CSWA 3, whilst the mass estimates come from our modelling described below.

To investigate the influence of environment, Fig. 3 shows $80' \times 80'$ grey-scale images of the number density of galaxies detected by SDSS, together with a $8' \times 8'$ zoom-in on the lens. To study the immediate neighbours of the lens galaxy, we use the SDSS photometric redshifts, as shown in the upper right panel. By cutting the distribution around the redshift of the lens, we build a luminosity function. Most of the lensing galaxies lie in poor groups with ~ 20 members, rather than rich clusters. In all cases, the lens galaxy is the brightest by 1 or 2 magnitudes in r.

2.3 Modelling of the Lenses

As a simple and flexible tool for modelling, we take advantage of the publicly available `PixeLens` [3] code (Saha & Williams 2004). Here, the mass distribution is pixellated into tiles. It is easy to find many possible mass tilings that reproduce the positions of the images exactly. `PixeLens` overcomes this problem by restricting attention to mass distributions for which (i) the density gradient anywhere must point within 45° of the centre, (ii) the projected density of any pixel must be less than twice the average value of its neighbors and (ii) the surface density radial profile $\kappa(r)$ must be steeper than $r^{-0.5}$. These constraints guarantee that the model is centrally concentrated, reasonably smooth and roughly isothermal $\kappa \sim r^{-1}$. The models always reproduce the relative positions of the lensing galaxies and the images, as listed in Table 2 of the images exactly, and they predict the psoitions of fainter additional images.

[2] http://users.ociw.edu/peng/work/galfit/galfit.html
[3] http://www.qgd.uzh.ch/projects/pixelens/

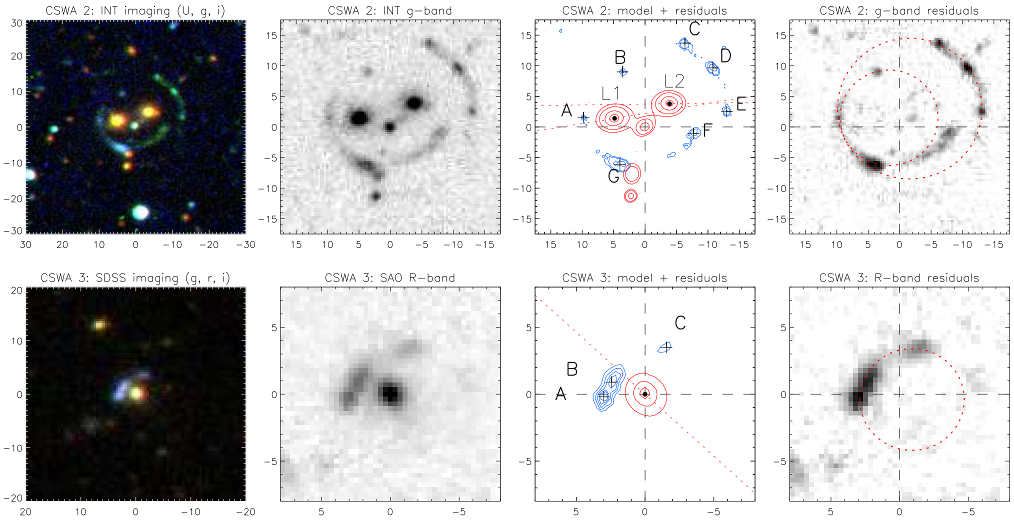

Figure 2. Left: Best available RGB composite (either SDSS or follow-up) for CASSOWARY lenses. Middle: Zoom-in of g (R) band image for CSWA 2 (CSWA 3). Right: GALFIT model to lens population (red) and residual after model subtraction (blue).

Parameter	CSWA 1 Cosmic Horseshoe	CSWA 2 Cheshire Cat	CSWA 3
α_L	11:48:33.1	10:38:47.95 10:38:39.20	12:40:32.28
δ_L	19:30:03.2	48:49:17.9 48:49:20.3	45:09:02.9
z_L	0.444	0.426 0.432	0.274
z_S	2.379	0.97 > 1.4	0.725
$(g,i)_L$	20.8,18.2	20.2, 17.9 20.5, 18.1	19.6, 17.8
$R_{\rm eff}$	1.7″	1.7″ 1.9″	2.4″
$(g,i)_S$	20.1,19.7	21.5, 20.6 21.0, 20.5	19.7, 19.3
R_E	5.1″	7.8″ 11.5″	3.8″
$M_E/10^{12}M_\odot$	5.4	17.7 33	2.4

Table 1. Observed and derived properties of the CSWA 2 and 3 lenses. The data on CSWA 1 from Belokurov et al. (2007) is shown for comparison.

3 CSWA 2, THE CHESHIRE CAT

CSWA 2, which we nickname "The Cheshire Cat" (Carroll, 1866), is a complicated lens system. The Cat's eyes are two giant early-type galaxies, which are probably responsible for most of the lensing effect. Our images are centered on the Cat's nose at $\alpha = 10:38:43.10, \delta = +48:49:16.50$, which is most likely a foreground object. The southern arc, which is the Cat's smile, is the brightest arc in the system and is clearly visible in the SDSS imaging. Given this complexity, we obtained some deeper multiband imaging with the INT, and integral field and long slit spectroscopy with the Calar Alto 3.5m and the WHT.

The INT observations were carried out on 2007 May 12/13 with the Wide Field Camera (WFC). The exposure times were 600 s in each of the three wavebands U, g and i – which are similar to the SDSS filters. The measured seeing (FWHM) on the images (0.33″ pixels) was 1.30″, 1.26″ and 1.21″ in U, g and i respectively. The INT data are roughly a magnitude deeper than the SDSS data and were reduced using the pipeline toolkit of Irwin & Lewis (2001). These were used to make the image shown in the top left of Fig. 2. The arcs are more extended than in the SDSS cut-out, with at least 7

Lens ID	Column vectors of Names, $\Delta\alpha$ offsets, $\Delta\delta$ offsets
CSWA 2	L_1, L_2, A, B, C, D, E, F, G (4.8, -4.05,9.7, 3.4, -6.45, -10.9, -13.1, -7.8, 3.9) (1.2, 3.75,1.4, 9., 13.7, 9.65, 2.5, -1.1, -6.2)
CSWA 3	L, A, B, C (0.00, 3.00, 2.45, -1.55) (0.00,-0.20, 0.90, 3.50)

Table 2. Locations of the images (A,B,C and so on) and the lensing galaxies (L_1, L_2) in arcseconds for CSWA 2 and CSWA 3.

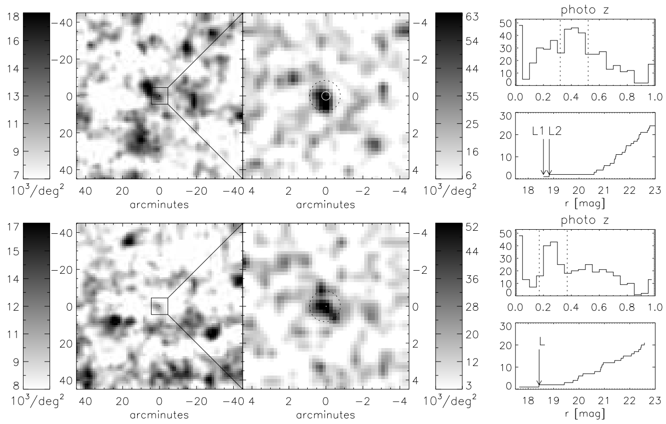

Figure 3. Density of galaxies in the vicinity of each lens with corresponding redshift range marked. Left: Large scale structure. Middle: Zoom-in on the lens marked by white ring, shown to scale. Right: Redshift distribution (upper panel) for all galaxies in the dashed circle in the middle panel. For galaxies in the range marked, we build the r-band cumulative LF of the group members (lower panel). The lens magnitude is shown with an arrow.

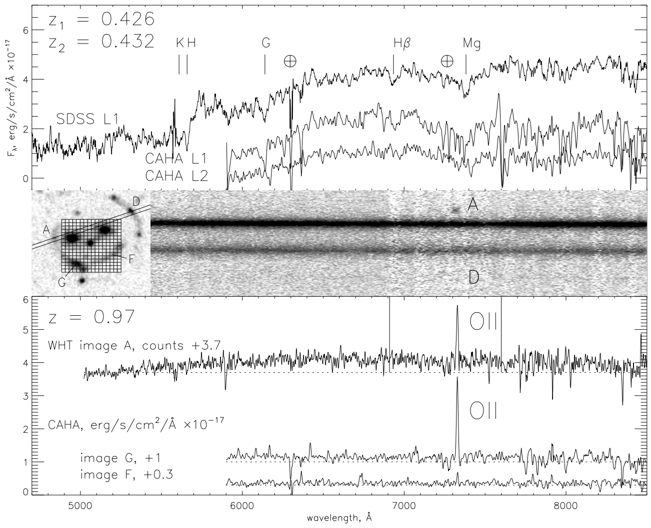

Figure 4. Spectroscopic data of CSWA 2 from SDSS, Calar Alto and the WHT. The top panel shows spectra of the two lens galaxies from SDSS and Calar Alto PMAS. Both galaxies exhibit features typical of early-type galaxies, including Ca K, H and G band absorption lines. Note that the two galaxies are at slightly different redshifts, $z_1 = 0.426$ and $z_2 = 0.432$. The $\oplus$ symbols mark the location of some prominent atmospheric absorption. The middle left panel shows the ISIS slit position and the PMAS IFU location. The middle right panel an extract of the ISIS 2D spectrum with distance along the slit plotted vertically and wavelength plotted horizontally. It is a zoom-in about the [O II] λ3728 and covers $\sim$ 30″ to span image A and D. The lower panel shows WHT and Calar Alto spectra of the arcs. In the PMAS data, we see prominent [O II] emission in G, but not in F. Similarly, in the ISIS data, the [O II] emission is clearly visible in the 2D cutout, as well as the 1D extracted spectrum, but there is no corresponding emission at the location of D. Images A, G and probably B are produced by a source at redshift $z = 0.97$, whilst D, F and most likely C and E are at a higher redshift.

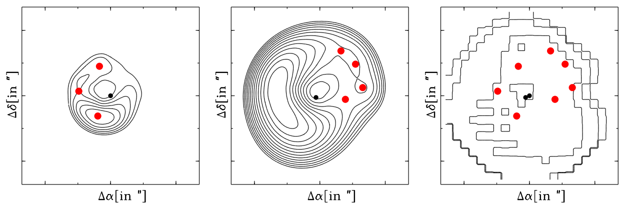

Figure 5. A `PixeLens` model of CSWA 2 with image locations (red dots) and source locations (black dots). The left and middle panels show the Fermat surface for the $z = 0.97$ and $z = 1.4$ sources respectively, the right panel shows the pixellated mass distribution. Note that for each source there are predicted additional images.

resolved bright knots visible. Moreover, the arc connecting A and B together with the knot G are bluer than the arcs connecting C, D, E and F (see the top panel in the third column for the nomenclature). This hints at the possibility of more than one source at more than one redshift for the Cheshire Cat.

Calar Alto observations were performed using the Potsdam Multi-Aperture Spectrophotometer (PMAS, Roth et al. 2005), at the 3.5m telescope on 2007 May 10/11. PMAS is an integral field spectrograph that comprises a lens array with 256 individual lenses. They sample the sky in a regular square grid of 16×16 elements, each with an individual field-of-view of 1″ in the selected configuration. A low-resolution grating (V300) giving a FWHM resolution of $\sim$7Å was used, covering the wavelength range 5780-9125Å. An exposure of 3600 s was taken on the central parts of CSWA 2, which included both lensing galaxies and the brightest knot in the southern arc. The data were then reduced using R3D (Sánchez et al. 2006), following the standard steps for fibre-based integral field spectroscopic data. The reduction steps include bias and pixel-to-pixel transmission correction, spectra tracing and extraction, wavelength calibration, fibre-transmission difference corrections and flux calibration. Once reduced, the frames were sky subtracted using E3D (Sánchez et al. 2004), by selecting the spectra corresponding to fibres free of object signal within the field-of-view. The resulting median sky spectrum was the subtracted for all fibres. After this final step, the spectra were reordered using the PMAS position table to create a final datacube.

Finally, a long-slit spectrum of knots A and D was obtained using the ISIS spectrograph on the WHT on the night of 2008 May 23. The observations were obtained as part of the WHT Service Programme in less than ideal conditions of high humidity, with variable seeing around 1.6″. The ISIS spectrograph was configured with the 5300Å dichoic and gratings R300B (blue arm) and R158R (red arm). A slit-width of 1.5″ was employed and a total on-sky exposure time of 4500 s was obtained, divided into five individual exposures of 900 s. Wavelength calibration was performed using exposures of standard calibration lamps. In practice, no useful information was obtained from the blue arm, but the data from the red arm provided wavelength coverage of 5300 – 10000 Å with a resolution of $\simeq$12Å FWHM. The data were obtained without any on-chip binning and the spatial scale along the slit was 0.22″per pixel. Standard reduction procedures were followed using IRAF[4] routines. The five individual object exposures were then combined, employing a sigma–clipping algorithm to eliminate cosmic-rays, and the spectra of the two central galaxies extracted. The spectrum-trace of the brighter galaxy was then repositioned along the slit to extract spectra of the two arc components A and D.

Fig. 4 summarises the available spectroscopic data on this object. The inset in the middle panel shows the placings of the PMAS IFU and the WHT long slit. The top panels shows the spectra for the lensing galaxy L_1 (SDSS and Calar Alto) and L_2 (just Calar Alto), which are typical of early-type galaxies, with Ca K, H, and G band lines, together with H_β. It is evident that L_1 and L_2 lie at slightly different redshifts, namely $z_1 = 0.426$ and $z_2 = 0.432$, which correspond to a separation of 14.3 Mpc in the standard cosmology ($\Omega_\mathrm{m} = 0.3, \Omega_\Lambda = 0.7, h = 0.7$.) It is also worth noting that L_2 is a radio source as detected by FIRST with 6.9 mJy flux. As regards the source, we have taken spectra of knots A and D with ISIS, and F and G with PMAS. The 2D ISIS spectra are shown in the middle panel and the 1D spectra from both ISIS and PMAS are shown in the lower panel. The main feature is the two strips in the middle of the 2D cut-out corresponding to the continuum of the lensing galaxies. Also visible in the range 6915 - 7600 Å is the narrow emission line [O II] λ3728 from a source at $z = 0.97$. As evident from the 2D spectra, the emission feature is not detected at the location of the D image. This is corroborated by the PMAS data in the lower panels, with G exhibiting strong [O II], but not F (although the signal from F is weak and so the evidence is perhaps not conclusive). Given the

[4] IRAF is distributed by the National Optical Astronomy Observatories, which are operated by the Association of Universities for Research in Astronomy, Inc. under cooperative agreement with the National Science Foundation.

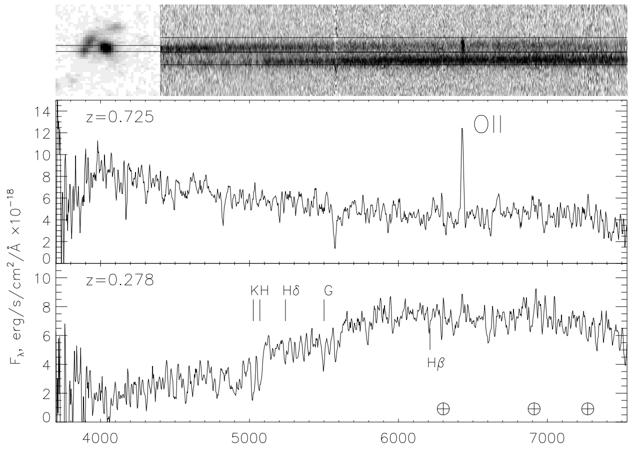

Figure 6. Spectroscopic follow-up of CSWA 3. The top panel shows the slit position and the 2D spectrum from the SAO SCORPIO Instrument. The 1d spectra are extracted from the regions marked and shown in the lower two panels. For the source, there is an unambiguous detection of the [O II] line at $z = 0.725$. The lens spectra is typical of an early-type galaxy with Ca H and K lines clearly visible, which puts the lens at redshift $z = 0.278$. The $\oplus$ symbols mark the location of prominent atmospheric absorption features.

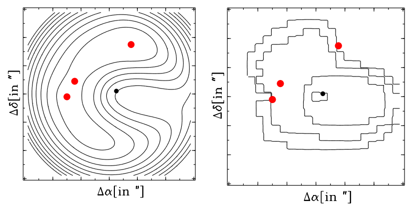

Figure 7. A `PixeLens` model of the CSWA 3 lens. The left panel shows the Fermat surface, the right panel the pixellated mass distribution. The image locations are shown as red dots, whilst the source location is shown as a black dot. Note that there is a predicted fourth image at the saddle of the Fermat surface.

absence of [O II] up to ~ 9300 Å in the ISIS spectra, we conclude that the redshift of the second source is likely in excess of $z = 1.4$.

A `PixeLens` model for CSWA 2 is shown in Fig. 5. The left and middle panels show the Fermat surfaces for the sources at $z = 0.97$ and $z = 1.4$ respectively, (although the latter is just a lower limit). The image locations of G, A and B are reproduced, together with a predicted faint counterimage offset from the centre by $\Delta\alpha \approx -3'', \Delta\delta \approx 6''$. The magnification of the $z = 0.97$ source is ~ 15. Similarly, for the higher redshift source, the images of C,D, E and F are reproduced, together with a predicted faint counterimage at $\Delta\alpha \approx -13'', \Delta\delta \approx 0''$. The magnification is ~ 45. Note that the density contours are roundish but with evident substructure, whilst the mass enclosed $M_{\rm E}$ within the outer ring of radius 11.5″ is a stupendous 33×10^{12} $M_\odot$ – almost a magnitude greater than the mass in the entire Local Group!

4 CSWA 3

Long-slit spectral observations of CSWA 3 were performed on 2008 March 28/29 with the multi-mode focal reducer SCORPIO (Afanasiev & Moiseev 2005) installed at the prime focus of the BTA 6-m telescope at the SAO in modest seeing (1.1″). The slit was placed to include some of the light from the lens galaxy, as shown in the inset of Fig. **??**. We used the VPHG550G grism which covers the wavelength interval 3650–7550 Å with a spectral resolution 8-10 Å FWHM. With a CCD EEV 42-40 2k × 2k detector, the reciprocal dispersion was 1.9 Å per pixel. The total exposure time was 1800 s, divided into two 900 s exposures. The target was moved along the slit between exposures to ease background subtraction and CCD fringe removal. The bias subtraction, geometrical corrections, flat fielding, sky subtraction, and calibration to flux units (F_λ) was performed by means of IDL-based software. From its spectrum, the source is a typical star-forming galaxy, with a redshift of $z = 0.725$, as judged from the prominent [O II] lines. There are no other viable redshift identifications given the lack of additional emission features in the spectrum. We also measured the lens redshift (which was unavailable in SDSS) from the Calcium K and H lines. The lens is an early-type galaxy at a redshift of $z = 0.278$.

CSWA 3 lies in a known galaxy cluster, namely NSCS J124034+450923, as identified in the DPOSS survey by Lopes et al. (2004). The cluster itself is a ROSAT detected X-ray source. CSWA 3 is probably a quadruplet, with the faintest image missing. To test this hypothesis, we build a `PixeLens` model, as shown in Fig. 7. The arc (or at least what we see of it) is quite circular, hinting that shear from the galaxy cluster plays a modest role. The lensing mass within the arc is ~ 2.4×10^{12} $M_\odot$ – consistent with most of the lensing effect coming from a single massive early-type galaxy. The magnification is ~ 16, with A and B as the most highly magnified images, followed by C. The model predicts a fourth image D, at the location of the saddle-point of the limacon in the Fermat time delay surface. Its predicted location is offset by $\Delta\alpha \approx -3'', \Delta\delta \approx -0.5''$ from the lens galaxy centre.

5 CONCLUSIONS

We have presented imaging, spectroscopy and modelling for two wide separation gravitational lenses. It is clear from the recent discoveries by the CASSOWARY group (Belokurov et al. 2007) and others (Allam et al. 2006; Shin et al. 2008) that there are a number of such lenses in the SDSS dataset. The two lenses we have discussed here are distinguished from among tens of candidates only by the fact that we have already obtained detailed spectroscopic and photometric follow-up. In our forthcoming survey paper, we plan to release the details of our search algorithm, together with a ranked list of our candidates (some already available at "http://www.ast.cam.ac.uk/research/cassowary/")

ACKNOWLEDGEMENTS

Funding for the SDSS and SDSS-II has been provided by the Alfred P. Sloan Foundation, the Participating Institutions, the National Science Foundation, the U.S. Department of Energy, the National Aeronautics and Space Administration, the Japanese Monbukagakusho, the Max Planck Society, and the Higher Education Funding Council for England. The SDSS Web Site is http://www.sdss.org/. We thank Pablo Rodriguez-Gil for undertaking the long-slit observations at the WHT. The WHT and its service programme are operated on the island of La Palma by the Isaac Newton Group in the Spanish Observatorio del Roque de los Muchachos of the Instituto de Astrofsica de Canarias. The paper is also based on observations collected at the Centro Astronḿico Hispano Alemán (CAHA) at Calar Alto, operated jointly by the Max-Planck Institut für Astronomie and the Instituto de Astrofísica de Andalucía (CSIC). The paper was partly based on observations collected with the 6m telescope of the Special Astrophysical Observatory (SAO) of the Russian Academy of Sciences (RAS) which is operated under the financial support of Science Department of Russia (registration number 01-43). A.V.M. also acknowledges a grant from the President of Russian Federation (MK1310.2007.2)"

REFERENCES

Afanasiev V. L., Moiseev A. V., 2005, AstL, 31, 194
Allam, S. S., Tucker, D. L., Lin, H., Diehl, H. T., Annis, J., Buckley-Geer,1 E. J., & Frieman, J. A. 2007, ApJ, 662, L51
Belokurov, V. et al 2007, ApJ, 671, L9
Carroll, L. 1866, Alice's Adventures in Wonderland, Macmillan, London
Dye, S., Evans, N. W., Belokurov, V., Warren, S. J., & Hewett, P. 2008, ArXiv e-prints, 804, arXiv:0804.4002
Eisenstein, D. J., et al. 2001, AJ, 122, 2267
Goto, T., et al. 2002, AJ, 123, 1807
Inada, N., et al. 2003, AJ, 126, 666
Irwin, M.J., Lewis, J.R., 2001, New Ast Rev, 45, 105
Johnston, D. E., et al. 2003, AJ, 126, 2281
Kubik, D. 2007, MSc thesis, Univ of Chicago
Lopes, P. A. A., et al. 2004, AJ, 128, 1017
Peng, C. Y., Ho, L. C., Impey, C. D., Rix, H.-W. 2002, AJ, 124, 266
Roth, M.M., Kelz, A., Fechner, T., et al., 2005, PASP, 117, 620
Saha, P., Williams, L. L. R. 2004, AJ, 127, 2604
Sánchez, S. F. 2004, AN, 325, 167
Sánchez, S. F. 2006, AN, 327, 850
Shin, E. M., & Evans, N. W. 2008, ArXiv e-prints, 804, arXiv:0804.3743
Shin, M.-S., et al. 2008, ArXiv e-prints, 804, arXiv:0804.1487
Werner, M. C., An, J., & Evans, N. W. 2008, ArXiv e-prints, 804, arXiv:0804.3744
Willis, J. P., Hewett, P. C., & Warren, S. J. 2005, MNRAS, 363, 1369